Electrical Engineering (2021) 103:1217–1237
https://doi.org/10.1007/s00202-020-01173-6

ORIGINAL PAPER

A new meta-heuristic programming for multi-objective optimal power flow

Fatima Daqaq[1,2] · **Mohammed Ouassaid**[1] · **Rachid Ellaia**[1,2]

Received: 7 February 2020 / Accepted: 25 November 2020 / Published online: 2 January 2021

Abstract

In this paper, a new multi-objective approach is suggested, known as multi-objective backtracking search algorithm (MOBSA) in order to formulate and solve the optimal power flow (OPF) problem in power systems. Many objective functions are considered like fuel cost, power losses, and voltage deviation. The structure of the proposed method is simple and has one control parameter. In addition, MOBSA is able to solve the highly constrained objectives. A fuzzy membership technique is integrated into the BSA algorithm to extract the best compromise solution from all the obtained Pareto optimal solutions. Furthermore, the capability of the MOBSA approach is evaluated and verified for bi- and tri-objectives, and tested on three standard IEEE power systems, small network 30-bus, medium network 57-bus, and large network 118-bus test systems. The obtained results reveal that the proposed method is efficient to generate well-distributed Pareto optimal non-dominated solutions. Likewise, the comparison analysis with some re-implemented methods as MODE, SPEA, MALO, and those found in the literature as MOABC/D, QOTLBO, NSGA-II and NSMOGSA, assured the superiority, effectiveness, and robustness of MOBSA.

Keywords Power system · Optimal power flow · Multi-objective optimization · Backtracking search algorithm · Fuzzy membership

List of symbols

a_i, b_i, c_i	Cost coefficients of the i^{th} generator
BCS	Best compromise solution
B_{ij}	Susceptance of the admittance matrix
D	Dimension
$f(x, u)$	Objective function
F	Scale factor
F_C	Fuel cost
G_{ij}	Conductance of the admittance matrix
$g(x, u)$	Equality constraints
$histPop$	Historical population
$h(x, u)$	Inequality constraints
low	Lower limits of problem
N	Population size (the number of individuals)
OPF	Optimal power flow
P_{gi}, P_{di}	Active and reactive power generated at i^{th} unit
P_{loss}	Power losses
Pop	Population
Q_C	Shunt VAR compensation
Q_{gi}, Q_{di}	Active and reactive power generated at i^{th} unit
S_{li}	Apparent power flow of i^{th} line
T_i	Tap settings of regulating transformer i
$T_{i,j}$	Trial population
u	Vector of independent variables or control variables
up	Upper limits of problem
VD	Voltage deviation
V_{gi}	Voltage magnitudes at i^{th} PV buses
V_{li}	Voltage magnitude at load bus i
x	Vector of dependent variables or state variables
μ_{fi}	Membership function of i^{th} objective

✉ Fatima Daqaq
fati.daqaq@gmail.com

Mohammed Ouassaid
ouassaid@emi.ac.ma

Rachid Ellaia
ellaia@emi.ac.ma

1 Engineering for Smart and Sustainable Systems Research Center, Mohammadia School of Engineers, Mohammed V University, Rabat, Morocco

2 Laboratory of Study and Research for Applied Mathematics, Mohammadia School of Engineers, Mohammed V University, Rabat, Morocco

θ_i	Voltage angles at i^{th} bus
BSA	Backtracking search algorithm
MALO	Multi-objective ant lion optimization
MDE	Multi-objective differential evolution
MICA3	Modified imperialist competitive algorithm
MOABC/D	Multi-objective artificial bee colony algorithm based on decomposition
MODE	Multi-objective differential evolution
MOO	Multi-objective optimization
NSMOGSA	Non-dominated sorting multi-objective gravitational search algorithm
NSGA II	Non-dominated sorting genetic algorithm
SPEA	Strength Pareto evolution algorithm
QOTLBO	Quasi-oppositional teaching learning-based optimization

1 Introduction

Power flow (PF) is becoming one of the most fundamental issues in power system, and the basic idea of the PF analysis which is also known as load flow analysis is to find out the voltage at different buses, power injection on lines, and total system power losses for any given operating conditions. Additionally, the optimal power flow (OPF) is a nonlinear, non-convex, and large-scale problem, which leads to optimize several objective functions by determining optimum settings of control variables, and satisfying a set of equality and inequality constraints. Generally, the control variables set contains the generator real powers, voltages of generation buses, tap setting of regulating transformers, and reactive power of shunt capacitors, whereas the objective functions were formulated as decreasing the total fuel cost, active power losses, and voltage deviation. The first authors who introduced the formulation of the OPF problem are Dommel and Tinney [1]. The popular numerical methods for solving the power flow equations are the Newton–Raphson (N-R) [2], Gauss–Seidel (G-S) [3], and fast decoupled (FD) methods [4].

Furthermore, the OPF problem can be solved via two kinds of methods, traditional and intelligent optimization algorithms. As traditional methods, several have been applied such as linear and nonlinear programming [5], quadratic programming [6], interior point method [7], and the ε-constraint methods [8]. However, those methods are usually slow in convergence, require heavy computational cost, and have multiple local minimum points. In earlier years, metaheuristic optimization methods are widely applied in searching for optimal solutions in large-scale problems of engineering, computer science, and business. They work by guiding the searching in a solution space to find the optimal. Those intelligent methods have been used for the global optimization problem. Numerous metaheuristic optimization techniques have been published lately such as black widow optimization (BWO) [9], salp swarm algorithm (SSA) [10], intensify harris hawks optimizer (IHHO) [11], hybrid harris hawks optimizer (hHHO-IGWO) [12], henry gas solubility optimization (HGSO) [13], hybrid grey wolf optimizer (hGWO) [14], manta ray foraging optimization (MRFO) [15], and so on. Recently, many researchers have tended to apply intelligent methods for solving the OPF problem such as differential evolution (DE) [16], ameliorated dragonfly algorithm (ADFA) [17], particle swarm optimization (PSO) [18], ant colony optimization (AC) [19], genetic algorithm (GA) [20], evolutionary algorithm (EA) [21], modified shuffle frog leaping algorithm (MSFLA) [22], gray wolf optimizer (GWO) [23], sine cosine algorithm (SCA) [24], and hybrid biogeography-based optimization (BBO) [25]. All the previous techniques have just considered single-objective OPF problems.

In recent years, several methods are applied to solve the multi-objective OPF problems (MOOPF). Generally, multi-objective optimal power flow problem is described as a highly large-scale and nonlinear constrained optimization. Among these methods, a modified artificial bee colony algorithm is developed, and the objectives are combined using fuzzy logic to form one single-objective function [26]. A decomposition-based memetic algorithm for multi-objective capacitated arc routing problem is improved [27]. An improved artificial bee colony algorithm based on Pareto is presented for solving the multi-objective dynamic optimal power flow problem [28]. An artificial bee colony algorithm based on decomposition (MOABC/D) in [29] is employed for multi-objective OPF. Ghasemi et al. [30] (Multi-objective optimal electric power planning in the power system using Gaussian bare-bones imperialist competitive algorithm) have attempted non-dominated sorting procedure to get a trade-off between two or more conflicting objectives simultaneously. An improved strength Pareto evolutionary algorithm is proposed to deal with the multi-objective OPF by considering the fuel cost and emission [31]. A quasi-oppositional modified Jaya algorithm is introduced for multi-objective optimal power flow [32]. A modified decomposition-based multi-objective OPF problem is solved with the consideration of different objectives [33]. A multi-objective harmony search algorithm is proposed to minimize fuel cost [34]. A highly constrained multi-objective OPF involving conflicting objectives is solved using a comprehensive learning particle swarm optimization (CLPSO) algorithm [35]. A modified flower pollination algorithm (MFPA) is implemented to calculate the PFs under different objective [36]. Multi-objective optimal power flow using differential evolution-based approach is presented in [37]. A novel differential evolution (MDE) solution methodology is investigated for multi-objective optimal power flow (MOPF) problem [38]. An enhanced differential evolution with self-adaptive strategy and mixed crossover operator is considered for MOOPF problem [39]. A multi-objective differential evolution algorithm (MODEA) based on forced initialization is suggested [40]. Imperialist competitive algorithm with some modified methods (MICA) is used to solve the MOPF problem using a Pareto-based approach [41].

In this paper, the analysis of power flow is established, and then, the study of the optimal power flow problem (OPF) is performed to optimize a particular objective functions while satisfying certain specified constraints (equality and inequality constraints). We emphasize on the development of optimal power flow technique using a multi-objective backtracking search algorithm (MOBSA). This latter is a methodology that seeks to find the solution of a group of objective functions. There are several objectives which must be optimized simultaneously, and they are different, i.e. when the first function diminished, the second increased and vice versa. Then, we should reach a compromise solution between two or more objectives. Backtracking search algorithm (BSA) is a stochastic optimization algorithm inspired from nature by Pinar Civicioglu [42]. Since it has been introduced, various researchers have tried to use the standard BSA due to its powerful global exploration, local exploitation, and high convergence speed. Other academics suggested new algorithms based on the original BSA in order to optimize its performance and its adaptability to different optimization problems. Moreover, BSA and its variants have been widely used in the field of engineering. It has been successfully performed in solving various real-world applications as follows: in material engineering, Ref [43] Chatzipavlis et all. proposed an approach called BSA-based neuro-fuzzy network, where the neuro-fuzzy network is used in the standard BSA for modelling the beach realignment, and to improve the performance of BSA, the authors modified its mutation and crossover in order to maintain a balance between exploration and exploitation. Control engineering: in [44], the authors suggested a shuffled BSA to identify the parameters of chaotic systems. In this novel method, two concepts were defined: firstly a new operator to initialize the trial population and secondly the population is separated to a several bunch. Afterwards, each group is developed by itself based on BSA process. After a repeated execution, a better search space exploration is provided and an independent search rises the exploitation capability of BSA. According to the recent study [45], an optimization of the output weights of deep stochastic configuration networks (DSCN) to construct optimal prediction intervals (PIs) is treated. Based on this, BSA was modified by proposing a dynamic updating strategy for the control factor (F), and a new adaptive mutation process to enhance its convergence. In addition, owing to the high number of variables to be optimized, a levy flight is adopted to produce another trial population to improve the diversity of a population. Mechanical engineering: in this study [46], a nonlinear active noise control system (ANC) is solved by a hybrid BSA with sequential quadratic programming SQP. This last was utilized with the BSA algorithm to enhance the search capabilities of BSA. In another study [47], a diagnosed gear fault is exploited using a support vector machine (SVM) optimization based on BSA (BSA-SVM). The efficiency of SVM is influenced by its optimal parameters. On this basis, BSA is included to make the optimization for the SVM parameters. Electrical engineering: as stated in [48], the maximum power point tracking (MPPT) is combined with BSA to analyse the I-V and P-V characteristics of different solar PV array configurations. The research in [49] introduced a binary backtracking search algorithm (BBSA) to find the optimal scheduling controller of microgrids virtual power plant. Referring to [50], the ORPD problem was solved by minimizing power losses, and improving the voltage profile using the BSA optimization. The authors of [51] applied backtracking search optimization algorithm (BSA) to perform the OPF calculation with non-smooth cost functions. Reference [52] solves multi-type distributed generators along distribution networks problems using a multi-objective BSA algorithm based on a weighting factor approach. Information and communication technology: as proposed in [53], a hybrid backtracking search with hyper-heuristic was utilized for minimizing the flexible job shop-scheduling problem (FJSPF) with fuzzy processing time. In BS-HH, BSA is used as the high-level strategy to find the optimal performing heuristics that generates near-optimal solutions for the FJSPF by using an efficient low-level heuristics. As articulated in [54], BSA was introduced to a dynamic QoS for maximizing the composite service quality in IoT application layer, to make a balance between the performance and computational time. All the experiment results of those previous optimization problems revealed an improved and robust performance of BSA approach. The remaining paper is organized in four sections as follows: Sect. 2 introduces mathematical model of multi-objective optimal power flow. Section 3 is focused on the explanation of the proposed multi-objective backtracking search algorithm method. The simulation results and discussion of MOBSA are demonstrated in the last section, and then, the paper will be finished by giving a short conclusion.

2 Multi-objective optimal power flow study

In general, the goal of a multi-objective optimal power flow (MOOPF) problem is to optimize two or more selected objective functions through optimal power system control parameters, while satisfying several equality and inequality constraints, simultaneously. It can be mathematically formulated as follows:

$$
\begin{aligned}
&Minimize : f(x,u) = f_1(x,u), f_2(x,u), ..., f_{N_{obj}}(x,u) \\
&Subject\ to : g(x,u) = 0 \\
&\qquad\qquad h(x,u) \leq 0
\end{aligned}
\tag{1}
$$

where $f(x, u)$ is the objective function to be optimized, $g(x, u)$ is the equality constraints, $h(x, u)$ is the inequality constraints, x is the vector of dependent variables (state variables), and u is the vector of independent variables (control variables).

2.1 State variables

The state variables x can be expressed as:

$$x^T = [P_{g1}, V_{L1}, ..., V_{LNpq}, Q_{g1}, ..., Q_{gNg}, S_{l1}, ..., S_{lNl}] \tag{2}$$

where P_{g1} is the generator active power output at slack bus, V_L is the load bus voltage magnitude at PQ buses, Q_g is the generator reactive power output of all generator units, and S_l is the transmission line loading (or line flow). N_{pq}, N_g and N_l denote the number of load buses, number of generating units, and number of transmission lines, respectively.

2.2 Control variables

The control variables u can be expressed as:

$$
\begin{aligned}
u^T = [&P_{g2}, ..., P_{gNg}, V_{g1}, ..., V_{gNg}, Q_{c1}, ..., \\
&Q_{cNc}, T_1, ..., T_{NT}]
\end{aligned}
\tag{3}
$$

where P_g is the active power generation at the PV buses except at the slack bus, V_g is the generation bus voltages magnitude at PV buses, T is the transformer tap settings, Q_c is the shunt VAR compensation, N_g, N_c and N_T are the number of generators, number of regulating transformers, and number of VAR (shunt) compensators, respectively.

2.3 Objective constraints

The optimal power flow problem has both equality and inequality constraints.

2.3.1 Equality constraints

The equality constraints are represented by the power balance equations defined as follows:

$$
\begin{cases}
P_{gi} - P_{di} - |V_i| \sum_{j=1}^{Nb} |V_j| [G_{ij} cos(\theta_{ij}) + B_{ij} sin(\theta_{ij})] = 0 \\
Q_{gi} - Q_{di} - |V_i| \sum_{j=1}^{Nb} |V_j| [G_{ij} sin(\theta_{ij}) + B_{ij} cos(\theta_{ij})] = 0
\end{cases}
\tag{4}
$$

where N_b is the number of buses, P_g is the active power generation, Q_g is the reactive power generation, P_d is the active load demand, Q_d is the reactive load demand, G_{ij} and B_{ij} are the elements of the admittance matrix $Y_{ij} = G_{ij} + jB_{ij}$ representing the conductance and susceptance between bus i and bus j, respectively, $\theta_{ij} = \theta_i - \theta_j$ is the difference in voltage angles between bus i and bus j.

2.3.2 Inequality constraints

The inequality constraints are the operating limits of the equipment present in the power system, and they are presented as:

– Generator constraints:

$$V_{gi}^{min} \leq V_{gi} \leq V_{gi}^{max} \quad i = 1, ..., Ng \tag{5}$$

$$P_{gi}^{min} \leq P_{gi} \leq P_{gi}^{max} \quad i = 1, ..., Ng \tag{6}$$

$$Q_{gi}^{min} \leq Q_{gi} \leq Q_{gi}^{max} \quad i = 1, ..., Ng \tag{7}$$

where V_i^{min} and V_i^{max} are, respectively, the minimum and maximum limits of the i^{th} bus voltage of power plant V_i. P_{gi}^{min} and P_{gi}^{max} are the maximum and minimum active power limit of the i^{th} generator. Q_{gi}^{min} and Q_{gi}^{max} represent the minimum and maximum reactive power limit of the i^{th} traditional generator, respectively. Ng is the number of generation.

– Transformer constraints:

$$T_i^{min} \leq T_i \leq T_i^{max} \quad i = 1, ..., N_T \tag{8}$$

where T_i^{min} and T_i^{max} represent the minimum and maximum limit of the i^{th} tap changer transformer T_i, respectively. N_T is the number of tap changers.

– Shunt VAR compensators constraints:

$$Q_{ci}^{min} \leq Q_{ci} \leq Q_{ci}^{max} \quad i = 1, ..., Nc \tag{9}$$

where $Q_{c,i}^{min}$ and $Q_{c,i}^{max}$ are the minimum and maximum limit of the i^{th} shunt compensator $Q_{c,i}$. Nc is the number of capacitor components connected to the power system.

– Security constraints:

$$V_{Li}^{min} \leq V_{Li} \leq V_{Li}^{max} \quad i = 1, ..., Npq \tag{10}$$

$$S_{li} \leq S_{li}^{max} \quad i = 1, ..., Nl \tag{11}$$

where S_{li} and S_{li}^{max} is the maximum limit of MVA of the i^{th} transmission line. Nl is the number of transmission lines of the power system.

2.4 Objective functions

Optimizing the fuel cost is frequently the most common objective function considered in the optimal power flow problem, and it is conventionally modelled by a quadratic equation. In addition, other important objectives are provided herein as power losses and voltage deviation.

2.4.1 Minimization of Total Fuel Cost

The fuel cost for each power plant can be expressed as follows [37]:

$$F_1 = F_c = min\left\{ \sum_{i=1}^{Ng} f_i(P_{gi}) \right. \\ = min\left\{ \sum_{i=1}^{Ng} c_i + b_i P_{gi} + a_i P_{gi}^2 + |d_i sin(e_i(P_i^{min} - P_{gi}))| \right. \quad (12)$$

where Ng is the number of generation. a_i, b_i, c_i, d_i, and e_i are the cost coefficients of generating unit i.

2.4.2 Active power losses (Ploss)

The power loss is one of the important objectives of the OPF problem, and it is expressed as [37]:

$$F_2 = P_{loss} = min\left\{ \sum_{i=1}^{N_l} G_i(V_i^2 + V_j^2 - 2V_i V_j cos(\delta_{ij})) \right. \quad (13)$$

where P_{loss} is the total active power losses of the transmission network. G_i is the transfer conductance.

2.4.3 Voltage deviation (VD)

Voltage deviation is a measure of voltage quality in the network. The bus voltage is considered as one of the most important security and service indexes. The aim of this objective function is to minimize all PQ bus voltage deviations from 1.0 p.u. Mathematically, it is expressed as [30]:

$$F_3 = VD = min\left\{ \sum_{i=1}^{Npq} |V_{Li} - 1.0| \right. \quad (14)$$

where VD is the total voltage magnitude deviation of the power system.

3 Multi-objective backtracking search algorithm

BSA is a population-based iterative evolutionary algorithm designed to be a global minimizer. This method is effective and capable of solving different numerical optimization problem (nonlinear, non-convex, and complex). Its structure is simple, and it needs just one control parameter unlike a lot of other search algorithms. BSA can be divided into five evolutionary mechanisms (Initialization, Selection I, Mutation, Crossover, and Selection II), and BSA's algorithm is summarized in Fig. 1.

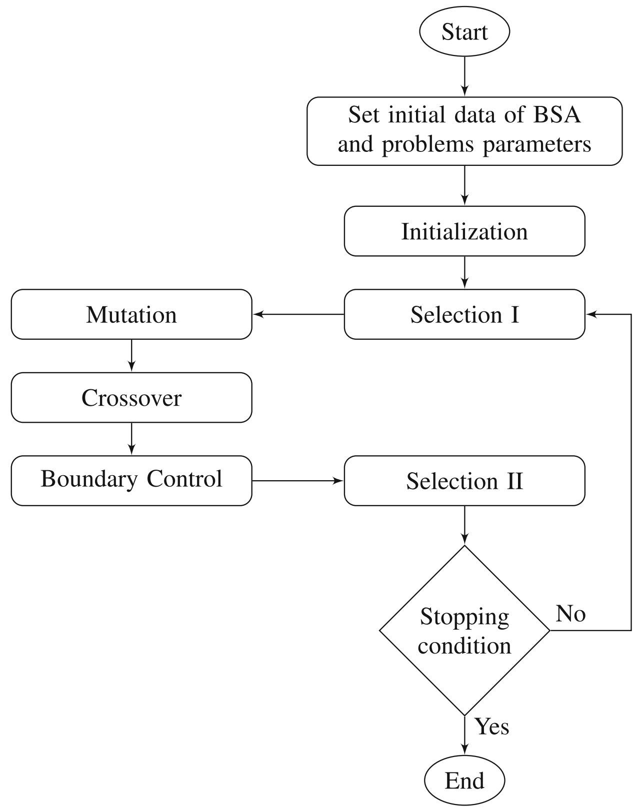

Fig. 1 Flow chart of the BSA algorithm

3.1 Backtracking Search Algorithm

The five major steps of BSA are described briefly herein:

Step 1: Initialization

The BSA method starts by initializing randomly two populations in the search space, named Pop and $histPop$, Eq. (15) and (16).

$$Pop_{i,j} = low_j + rand[0,1].(up_j - low_j) \quad (15)$$

$$histPop_{i,j} = low_j + rand[0,1].(up_j - low_j) \quad (16)$$

where Pop and $histPop$ are the current and historical populations, respectively. $i = 1, \ldots, N$ and $j = 1, \ldots, D$ are the population size and dimension of the problem, respectively. $rand$ is a uniform distribution between 0 and 1. The algorithm of this step is shown in Algorithm 1.

Algorithm 1. Initialization step of BSA

```
Input: N,D,low,up
Output: Pop
 for i = 1:N
  for i = 1:D
    Pop(i,j) = rand*(up(j) - low(j)) + low(j);
    histPop(i,j) = rand*(up(j) - low(j)) + low(j);
  end
 end
```

Step 2: Selection I

$histPop$ is generated at the beginning of each iteration following the rule of $(if - then)$ according to Eq. (17):

$$histPop = \begin{cases} Pop, & if \ \ (a \prec b | a, b - U(0,1)) \\ histPop, & otherwise \end{cases} \tag{17}$$

After determining the $histPop$, a permuting function (random shuffling function) is used to change randomly the order of the individuals in $histPop$ using Eq. (18).

$$histPop := permuting(histPop) \tag{18}$$

Step 3: Mutation

Mutation operator initializes the form of trial population according to the following equation:

$$M = Pop + F.(histPop - Pop) \tag{19}$$

where F is a parameter controlling the amplitude of the search direction matrix computed as the difference between the historical and the current populations matrix ($histPop$ - Pop).

Step 4: Crossover

The final form of the trial population is determined in BSA's crossover. This process uses two steps: The first determines the number of elements of each individual by a control parameter named $mixrate$. The second generates a random binary matrix map with a same size of Pop Algorithm 2.

The parameter $mixrate$ controls the maximum number of elements in each row of matrix map with the value of 1.

$$V_{i,j} = \begin{cases} Pop_{i,j} & if \quad map_{i,j} = 1 \\ M_{i,j} & otherwise \end{cases} \tag{20}$$

– Boundary Control Mechanism of BSA:

After the crossover, some individuals might violate the boundaries of the optimization variables, so they need to be checked and modified by an appropriate mechanism Algorithm 3.

Algorithm 2. Crossover's step of BSA

```
Input: mutant, mixrate, N, D
Output: trialpopulation (T)
 map(1:N,1:D) = 1
 if rand ≺ rand
  for i = 1:N
    u = randperm(D)
    map(i, u(1 : ceil(mixrate * rand * D))) = 1
  end
  else
  for i = 1:N
    map(i,rand(D)) = 1
  end
 end
 for i = 1:N
  for i = 1:D
    if map_{i,j} = 1
      T := Pop_{i,j}
    end
  end
 end
```

Algorithm 3. Boundary Control Mechanism of BSA

```
Input : T, low_j, up_j
Output: T
 for i = 1:N
  for i = 1:D
    if (T_{i,j} ≺ low_j) or (T_{i,j} ≻ up_j)
      T_{i,j} = randast * (up_j − low_j) + low_j
    end
  end
 end
```

Step 5: Selection II

In this stage, BSA compares each individual of V with its homologue from Pop in order to determine the next population Pop.

$$Pop_i^{next} = \begin{cases} V_i & if \quad f(V_i) \preceq f(P_i) \\ Pop_i & otherwise \end{cases} \tag{21}$$

3.2 Proposed MOBSA non-dominated approach

The important phases in MOBSA are the two main steps, mutation and crossover mentioned previously.

As mentioned before, in each generation of the evolution process, BSA deals with the population Pop. The offspring population V is produced by the phase's mutation and crossover. And in the Selection II, the individuals of Pop and of V are compared. For improving BSA to multi-objective optimization application, the comparison needs to be modified according to the concept of Pareto dominance. When the individual Pop is compared with the individual V, three situations are occurred, in which the first V is selected as the individual of the next population, but the second and the third situations Pop are selected:

– Pop is dominated by V if $V \prec Pop$.

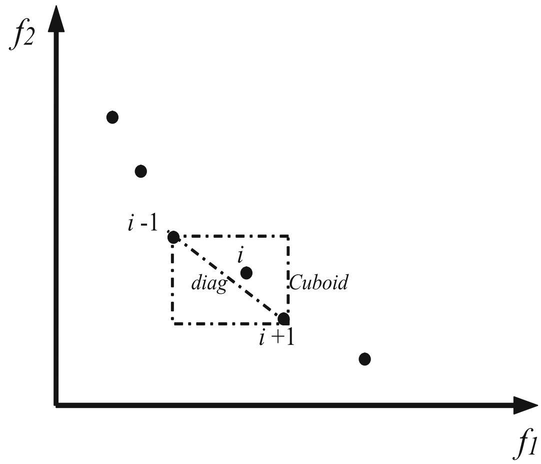

Fig. 2 Crowding distance calculation of the density estimation

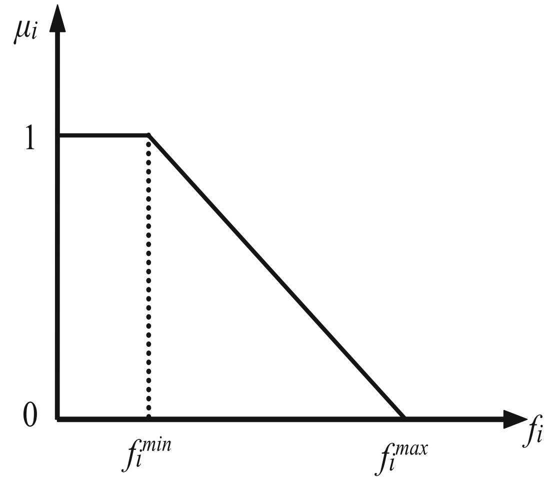

Fig. 3 Membership functions for objective function

- Pop dominates V if $Pop \prec V$.
- Neither Pop is dominated by V, nor Pop dominates V if $V \prec Pop$ and $Pop \prec V$.

3.2.1 Phases of multi-objective BSA

The steps of MOBSA are described as follows:

Step 1: Initialize two populations in the search space Ω (Pop and $histPop$) using Eqs. (15) and (16), and set the iteration number $i = 0$.

Step 2: Evaluate the fitness function of each individual of Pop and save the non-dominated solutions from among the population members into the non-dominated sorting.

Step 3: redefine the $histPop$ and modify it through Eqs. (17) and (18).

Step 4: the trial population M is generated by applying the mutation operator through Eq. (19).

Step 5: determine the final trial population V by the crossover step through Eq. (20). Then verify and modify the constraints.

Step 6: determine the next population Pop by comparing each individual of V with its homologue from Pop using Eq. (21).

Step 7: set $i = i + 1$ and then verify the stopping criteria, if algorithm needs to be repeated, return to Step 3.

3.2.2 Crowding distance

A specific crowding distance strategy is employed to define an ordering among individuals. The crowding distance value of a particular solution is the average distance of its two neighbouring solutions. The quantity D_p serves as an estimate of the diagonal of the cuboid formed by using the nearest neighbours as the vertices. To compute the crowding distance, we need to sort the population according to each objective function value in ascending order. Thereafter, for each objective function, the boundary solutions are assigned an infinite distance value. All other intermediate solutions are assigned a distance value equal to the corresponding diagonal length.

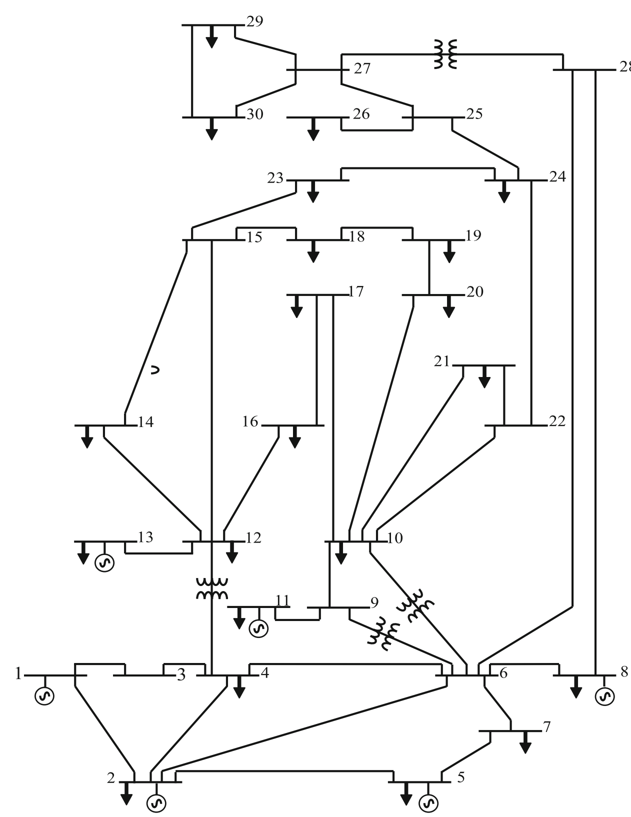

Fig. 4 Single line diagram of IEEE 30-bus test system

The crowding distance of the i^{th} solution in its front as the diagonal length of the cuboid is shown in Fig. 2.

Table 1 The characteristics details of the system

Systems	IEEE-30		IEEE-57		IEEE-118	
Characteristics	Value	Details	Value	Details	Value	Details
Buses	30	[57]	57	[58]	118	[58]
Branches	41	–	80	–	186	–
Generators	6	Buses: 1, 2, 5, 8, 11 and 13	7	Buses: 1, 2, 3, 6, 8, 9 and 12	54	Buses: 1, 4, 6, 8, 10, 12, 15, 18, 19, 24, 25, 26, 27, 31, 32, 34, 36, 40, 42, 46, 49, 54, 55, 56, 59, 61, 62, 65, 66, 69, 70, 72, 73, 74, 76, 77, 80, 85, 87, 89, 90, 91, 92, 99, 100, 103, 104, 105, 107, 110, 111, 112, 113 and 116
Shunts	9	Buses: 10, 12, 15, 17, 20, 21, 23, 24 and 29	3	Buses: 18, 25 and 53	14	Buses: 5, 34, 37, 44, 45, 46, 48, 74, 79, 82, 83, 105, 107, 110
Transformers	4	Branches: 11, 12, 15 and 36	17	Buses: 19, 20, 31, 35, 36, 37, 41, 46, 54, 58, 59, 65, 66, 71, 73, 76 and 13	9	Branches: 8, 32, 36, 51, 93, 95, 102, 107 and 127
Control variables	24	–	33	–	130	–

Table 2 Various case studies

			$Cost$	P_{loss}	VD
IEEE-30	Bi-Objective	Case 1	√	√	
		Case 2		√	√
	Tri-Objective	Case 3	√	√	√
IEEE-57	Bi-Objective	Case 4	√	√	
		Case 5		√	√
	Tri-Objective	Case 6	√	√	√
IEEE-118	Bi-Objective	Case 7	√	√	
		Case 8		√	√

3.2.3 The best compromise solution

The fuzzy logic term was first introduced and described using membership functions by L.A. Zadeh in 1965 [55]. It was elaborated to define the distinctions among data which is neither true nor false, which means that fuzzy logic aids to deal with the uncertainty of any situation and decide whether the statement is true or false. The only condition a membership function must really satisfy is that it must vary between 0 and 1. The fuzzy has been applied to various fields, from control theory to AI.

In this paper, once getting the non-dominated Pareto optimal set using the MOBSA approach, we may need to extract one optimal among the Pareto optimal solutions, which is called the best compromise solution, for satisfying the different goals to some extent. However, owing to the uncertainty of the decision maker's judgement in multi-objective optimization problems, a fuzzy decision-making strategy is integrated to tune this issue. For this purpose, each objective function f_i is mapped to [0,1] by linear membership function. Then, the fuzzy membership function for i^{th} objective function can be calculated as follows:

$$\mu_{fi} = \begin{cases} 1 & if \quad f_i \preceq f_i^{min} \\ \dfrac{f_i^{max} - f_i}{f_i^{max} - f_i^{min}} & if \quad f_i^{min} \prec f_i \prec f_i^{max} \\ 0 & if \quad f_i \succeq f_i^{max} \end{cases} \tag{22}$$

where i is the index of objective functions, μ_{fi} represents the membership function of i^{th} objective, f_i is the fitness value of i^{th} objective function, f_i^{min} and f_i^{max} are the minimum and maximum fitness value of i^{th} objective function among all the non-dominated solutions.

Therefore, the membership function represents the degree of membership in fuzzy sets using values between 0 and 1. The value 0 indicates incompatibility with the sets, while 1 means full compatibility Fig. 3. For each Pareto solution k,

Table 3 Cost coefficients

	Unit	Cost coefficients				
		a	b	C	d	e
		($/MWh2)	($/MWh)	($/h)		
IEEE-30	1	0.00375	2.00	0	18	0.037
	2	0.01750	1.75	0	16	0.038
	5	0.0625	1.00	0	14	0.04
	8	0.00834	3.25	0	12	0.045
	11	0.025	3.00	0	13	0.042
	13	0.025	3.00	0	13.5	0.041
IEEE-57	1	0.0775795	20	0	18	0.037
	2	0.01	40	0	16	0.038
	3	0.25	20	0	13.5	0.041
	6	0.01	40	0	18	0.037
	8	0.0222222	20	0	14	0.040
	9	0.01	40	0	15	0.039
	12	0.0322581	20	0	12	0.045
IEEE-118	1	0.01	40	0	–	–
	4	0.01	40	0	-	–
	6	0.01	40	0	–	–
	8	0.01	40	0	–	–
	10	0.0222222	20	0	–	–
	12	0.117647	20	0	–	–
	15	0.01	40	0	–	–
	18	0.01	40	0	–	–
	19	0.01	40	0	–	–
	24	0.01	40	0	–	–
	25	0.0454545	20	0	–	–
	26	0.0318471	20	0	–	–
	27	0.01	40	0	–	–
	31	1.42857	20	0	–	–
	32	0.01	40	0	-	-
	34	0.01	40	0	-	–
	36	0.01	40	0	–	–
	40	0.01	40	0	–	–
	42	0.01	40	0	–	–
	46	0.526316	20	0	–	–
	49	0.0490196	20	0	–	–
	54	0.208333	20	0	–	–
	55	0.01	40	0	–	–
	56	0.01	40	0	–	–
	59	0.0645161	20	0	–	–
	61	0.0625	20	0	–	–
	62	0.01	40	0	–	–
	65	0.0255754	20	0	–	–
	66	0.0255102	20	0	–	–
	69	0.0193648	20	0	–	–
	70	0.01	40	0	–	–
	72	0.01	40	0	–	–
	73	0.01	40	0	–	–
	74	0.01	40	0	–	–
	76	0.01	40	0	–	–
	77	0.01	40	0	–	–
	80	0.0209644	20	0	–	–
	85	0.01	40	0	–	–
	87	2.5	20	0	–	–
	89	0.0164745	20	0	–	–
	90	0.01	40	0	– -	-
	91	0.01	40	0	–	–
	92	0.01	40	0	–	—
	99	0.01	40	0	–	–
	100	0.0396825	20	0	–	–
	103	0.25	20	0	–	–
	104	0.01	40	0	–	–
	105	0.01	40	0	–	–
	107	0.01	40	0	-	–
	110	0.01	40	0	–	–
	111	0.277778	20	0	–	–
	112	0.01	40	0	–	–
	113	0.01	40	0	–	–
	116	0.01	40	0	–	–

the normalized membership function is defined as:

$$\mu^k = \frac{\sum_{i=1}^{m} \mu_{fi}^k}{\sum_{k=1}^{D} \sum_{i=1}^{m} \mu_{fi}^k} \tag{23}$$

where D is the number of non-dominated solutions, and m is the number of objective functions.

Now, the best compromise solution is the one that has the maximum value of minimum membership number μ^k, and it can be selected using the min-max method following the fuzzy decision process in [56] as follows:

$$\mu_{opt} = max\{\mu^k\} \tag{24}$$

4 Simulation results and discussion

Results analysis

To improve the effectiveness of the proposed algorithm for solving optimal power flow (OPF) problem, we applied it to a

Table 4 Obtained solutions for the IEEE 30-bus power system case 1

Control variables	MOBSA			MODE			SPEA			MALO		
	Cost	Loss	BCS	Cost	Loss	BCS	Cost	Loss	BCS	Cost	Loss	BCS
P_{g2}	48.475	79.988	55.423	47.565	76.835	50.619	46.401	76.875	57.386	51.26993	51.26999	51.26997
P_{g5}	21.845	50.000	33.502	20.148	49.772	34.480	20.091	49.983	35.866	25.99693	25.99691	25.99693
P_{g8}	20.804	34.914	35.000	23.950	34.994	34.722	32.116	34.976	34.887	27.12611	27.12610	27.12611
P_{g11}	11.511	30.000	30.000	13.723	29.484	29.552	11.401	29.982	29.692	20.79706	20.79707	20.79707
P_{g13}	12.000	40.000	24.377	12.196	36.173	24.422	12.044	39.890	22.844	21.34633	21.34632	21.34631
V_{g1}	1.0999	1.0999	1.0999	1.0996	1.0950	1.0999	1.0983	1.0996	1.0996	1.1000	1.1000	1.1000
V_{g2}	1.0887	1.0000	1.0928	1.0836	1.0867	1.0895	1.0810	1.0965	1.0919	1.092387	1.092388	1.092388
V_{g5}	1.0640	1.0855	1.0708	1.0580	1.0641	1.0674	1.0509	1.0760	1.0713	1.061487	1.061488	1.061488
V_{g8}	1.0701	1.0896	1.0804	1.0667	1.0717	1.0791	1.0675	1.0836	1.0802	1.084025	1.084024	1.084024
V_{g11}	1.1000	1.0817	1.0894	1.0926	1.0984	1.0987	1.0106	1.0849	1.0840	1.093276	1.093275	1.093275
V_{g13}	1.1000	1.0999	1.1000	1.0929	1.0943	1.0983	1.0770	1.0877	1.0842	1.061336	1.061336	1.061336
Q_{c10}	2.9764	5.0000	3.9273	4.9707	3.4706	3.2588	4.5427	4.9409	4.9387	2.109247	2.109248	2.109247
Q_{c12}	5.0000	3.6734	4.9732	1.3926	4.2595	4.6511	2.7997	4.5920	4.5703	2.966364	2.966364	2.966364
Q_{c15}	4.9854	4.3834	4.8344	4.5514	3.2474	4.5360	4.5294	4.6064	4.5643	3.995148	3.995148	3.995149
Q_{c17}	4.8436	5.0000	4.8246	3.3738	3.9712	4.2385	1.8016	4.5580	4.3218	3.417971	3.417972	3.417903
Q_{c20}	4.7549	4.5855	5.0000	3.7757	3.5806	4.5103	4.2068	4.1465	4.2076	3.779269	3.779267	3.779265
Q_{c21}	4.5295	5.0000	5.0000	4.6081	4.7287	4.5210	4.6988	4.7442	4.6706	4.526240	4.526240	4.526242
Q_{c23}	2.8563	2.4909	2.3493	4.9681	2.8489	3.4606	3.5628	4.9282	3.9641	1.423344	1.423345	1.423344
Q_{c24}	5.0000	4.9998	5.0000	4.2412	4.3352	4.6523	4.3545	4.8820	4.4381	2.378422	2.378423	2.378420
Q_{c29}	1.4107	2.0878	2.2667	1.4169	2.5013	2.4583	2.4875	4.4754	4.2840	3.536467	3.536469	3.536467
T_{11}	0.9669	1.0899	1.0127	1.0227	1.0182	1.0130	1.0173	1.0207	1.0157	1.065017	1.065017	1.065017
T_{12}	1.0112	0.9000	0.9764	0.9444	0.9064	0.9137	0.9850	0.9984	0.9947	1.084842	1.084842	1.084821
T_{15}	1.0127	1.0396	1.0124	1.0112	0.9888	0.9720	1.0401	1.0209	1.0203	1.094906	1.094906	1.094907
T_{36}	0.9712	0.9908	0.9787	0.9854	0.9657	0.9644	1.0083	0.9939	1.0082	1.085405	1.085405	1.085404
Fuel Cost ($/h)	**799.046**	966.766	843.468	799.476	949.248	841.386	801.165	960.271	848.243	801.567	952.523	852.300
P_{loss} (MW)	8.6168	**2.8841**	4.6336	8.4195	3.0456	4.7015	8.1644	2.9321	4.5461	8.4723	3.1869	4.6818

Bold values are show the results clearly found

three power systems, IEEE 30-bus in Fig. 4, IEEE 57-bus, and IEEE 118-bus test systems. Table 1 summarizes the characteristics details of these various systems. We considered eight different cases with different complexity illustrated by the cases reported in Table 2. The dimension (control variables) of OPF problem is 24, 33, and 130 for IEEE 30-bus, 57-bus, and 118-bus systems, respectively. The population size and maximum number of function evaluation are varied depending on the different cases. The cost coefficients of the three systems are included in Table 3. The results obtained by the proposed approach are compared with the results found by other heuristic methods as illustrated in the next subsection. The optimal settings of control variables found are shown in Tables 4, 6, 7, 8, 10, 12, 14, and 15.

The proposed MOPF optimization problem was solved using a computer with Intel Core i5 CPU @2.7 GHz and 4GB RAM. The simulation results were implemented in MATLAB R2016b software.

4.1 IEEE 30-bus power system

The IEEE 30-bus test system consists of 6 generators in which bus 1 is chosen as the slack bus, 24 load buses, 41 branches, 4 transformers, and 9 shunt reactive power injections as illustrated in Table 1. The optimization problem has 24 control variables, where its boundaries are taken between [0.95–1.1] for voltage magnitude, [0.9–1.1] for transformer taps, and [0–5] for VAR compensators. The detailed data (line and bus data) for the considered IEEE 30-bus system are given in [57]. The system active and reactive power demands are 283.4 (MW) and 126.2 (MVAR), respectively.

4.1.1 Case 1: fuel cost and power losses

For this case, the optimization of fuel cost and power losses is considered simultaneously as the multi-objective function of the OPF. The simulation was run using the proposed algorithm with NP = 100 and a maximum of 200 iterations.

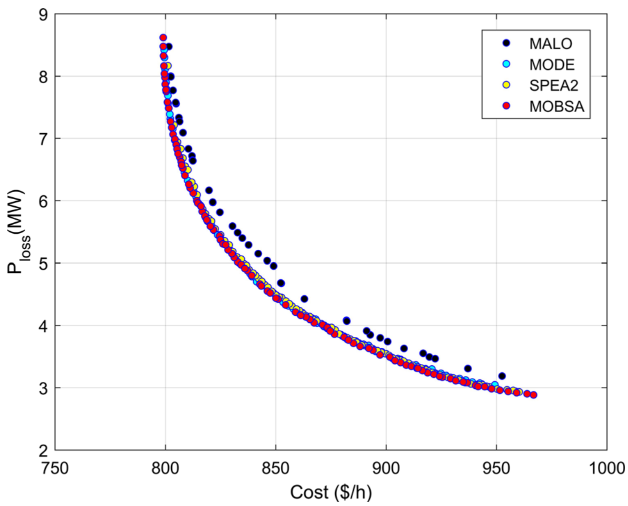

Fig. 5 Pareto fronts case 1

Figure 5 shows the Pareto front (non-dominated solution) for this case. The results obtained are presented in Table 4. The minimum fuel cost, minimum active loss, and the best compromise solutions obtained were 799.046 ($/h) and 2.8841 (MW), and (843.468 ($/h), 4.6336 (MW)), respectively. Table 5 provides the comparison between the results attained with other methods reported in the literature as MOABC/D, NSMOGSA, and NSGA-II.

4.1.2 Case 2: fuel cost, voltage deviation

In Case 2, minimization of fuel cost and voltage deviation is simultaneously considered. Simulation was run with NP = 100 and a maximum of 200 iterations. The simulation results of this case are shown in Table 6, and its Pareto front is illustrated in Fig. 6. The minimization result fuel cost and voltage values in this case are 799.298 ($/h) and 0.128 (p.u.), respectively. The BCS are 799.6455 ($/h) and 0.4182 (p.u.). Comparison analysis with other algorithms was also performed, and its results are illustrated in Table 6.

4.1.3 Case 3: fuel cost, power losses, and voltage deviation

This case shows the minimization of all objective functions (fuel cost, power losses, and voltage deviation) simultaneously. The proposed MOBSA gives best cost, best active losses, and best voltage deviation of 799.271 ($/h), 2.8589 (MW), and 0.0959 p.u. as given in Table 7, respectively. Figure 7 displays the Pareto front for this case, and Table 7 tabulates the comparison between the proposed method and others.

Table 5 Comparison solutions with other approaches for case 1

Approaches	Objective functions	Cost	Loss
MOBSA	Min Cost	**799.046**	8.6168
	Min Loss	966.766	**2.8841**
MODE	Min Cost	799.476	8.4195
	Min Loss	949.248	3.0456
SPEA	Min Cost	801.165	8.1644
	Min Loss	960.271	2.9321
MALO	Min Cost	801.567	8.4723
	Min Loss	952.523	3.1869
MOABC/D [29]	Min Cost	799.179	8.6446
	Min Loss	912.854	3.3714
NSMOGSA [59]	Min Cost	799.6095	7.9027
	Min Loss	873.5107	3.4925
NSGA II [34]	Min Cost	801.714	8.1734
	Min Loss	875.005	4.3571

Bold values are show the results clearly found

4.2 IEEE 57-bus power system

This test system has 7 generators (slack generator is at bus 1), 50 load buses, and 80 branches where 17 line OLTCs are existed, 15 transformers, 3 shunt reactive power injections, six generators real powers, and 7 generators voltages. This system has totally 33 control variables for OPF problem. The voltage magnitude limits are between 0.95 and 1.1 p.u. The lower and upper limits of transformer taps are 0.9 and 1.1 p.u., respectively. The limits of VAR compensators are varying between 0 to 20. Line and bus data are provided in [58]. Active and reactive power demands are 1250.8 (MW) and 336.4 (MVAr), respectively.

4.2.1 Case 4: fuel cost and power losses

The minimum fuel cost and losses values obtained in this case are 41623.292 ($/h) and 8.5788 (MW), respectively. And the BCS are 41959.152 ($/h) and 9.7667 (MW), its optimal control variables are tabulated in Table 8, and the Pareto front is shown in Fig. 8. This result is obtained for 200 generations, 400 iterations, and is compared with other methods as shown in Table 9.

4.2.2 Case 5: fuel cost and voltage deviation

The minimization of two objectives such as fuel cost and voltage deviation is considered simultaneously to solve the MOOPF problem. The non-dominated solutions obtained are given in Fig. 9. It is observed from Table 10 that the best compromise solution (BCS) attained is 41721.309 ($/h) and 0.6462 (p.u.), and the minimum of fuel cost and voltage is

Table 6 Obtained solutions for the IEEE 30-bus power system case 2

Control variables	MOBSA			MODE			SPEA			MALO		
	Cost	Loss	BCS	Cost	Loss	BCS	Cost	Loss	BCS	Cost	Loss	BCS
P_{g2}	48.4126	47.645	48.9836	48.970	48.9403	49.4573	49.9109	50.9868	48.7199	46.6996	46.6996	46.6997
P_{g5}	21.4633	19.886	21.1044	21.158	22.089	21.3037	21.0139	23.6908	21.0169	20.6716	20.6716	20.6716
P_{g8}	20.9497	21.265	21.2825	20.505	22.378	23.0516	21.6579	20.4698	21.6206	21.6290	21.6291	21.6291
P_{g11}	11.8331	13.448	11.5188	11.736	10.896	11.8079	11.6909	12.9040	11.8656	17.0743	17.0743	17.0743
P_{g13}	12.0540	12.007	12.000	12.207	13.258	12.0843	12.4247	12.4736	12.4486	14.1072	14.1073	14.1073
V_{g1}	1.1000	1.0570	1.1000	1.0979	1.0137	1.0597	1.0903	1.0352	1.0755	1.0703	1.0703	1.0703
V_{g2}	1.0879	1.0339	1.0835	1.0845	1.0248	1.0382	1.0692	1.0423	1.0574	1.0587	1.0587	1.0587
V_{g5}	1.0597	1.0024	1.0521	1.0581	1.0204	1.0064	1.0409	1.0169	1.0179	1.0310	1.0310	1.0310
V_{g8}	1.0688	1.0071	1.0589	1.0596	1.0053	1.0053	1.0444	1.0065	1.0259	1.0328	1.0328	1.0328
V_{g11}	1.1000	0.9500	1.0218	1.0761	1.0481	1.0404	1.0987	1.0009	1.0902	1.0468	1.0468	1.0468
V_{g13}	1.0593	1.0102	1.0441	1.0392	0.9892	1.0263	1.0574	0.9813	1.0123	1.0283	1.0283	1.0283
Q_{c10}	0.3012	1.8465	1.1213	1.2372	4.0436	2.9792	3.7411	2.8756	2.8726	2.8681	2.8681	2.8681
Q_{c12}	4.4434	4.9147	0.1941	1.6120	1.7462	2.8903	2.6759	2.2191	2.6771	2.8651	2.8651	2.8651
Q_{c15}	3.5952	5.0000	0.1918	4.1297	3.8994	1.6470	3.4735	2.7374	3.1781	3.0629	3.0629	3.0629
Q_{c17}	4.9784	4.8485	4.4628	2.8694	0.6220	1.7818	4.6616	3.3391	3.4798	3.3717	3.3717	3.3717
Q_{c20}	3.4688	5.0000	4.7729	3.5241	4.4082	4.0308	3.3764	4.1390	2.8724	2.8166	2.8166	2.8166
Q_{c21}	5.0000	5.0000	4.6199	4.1726	4.6130	3.6000	4.9920	4.8666	4.9160	3.5005	3.5005	3.5005
Q_{c23}	4.2940	4.3718	5.0000	3.1370	2.7306	4.7388	3.7577	4.5037	3.7590	1.9765	1.9765	1.9765
Q_{c24}	5.0000	5.0000	4.8674	4.2391	4.6533	4.9646	4.6972	4.9402	4.3955	3.9339	3.9339	3.9339
Q_{c29}	3.0237	4.1473	2.8969	2.2313	2.2595	3.2463	3.7933	3.2637	3.4298	3.0937	3.0937	3.0937
T_{11}	1.0748	0.9663	1.0558	1.0344	1.0527	1.0336	1.0400	0.9448	1.0236	0.9797	0.97979	9.7979
T_{12}	0.9909	0.9000	1.0070	1.0125	0.9073	0.9212	1.0422	0.9896	1.0521	1.0094	1.0094	1.0094
T_{15}	1.0614	0.9941	1.0798	1.0414	0.9246	1.0159	1.0168	0.9169	1.0069	0.9909	0.9909	0.9909
T_{36}	1.0202	0.9750	1.0238	1.0092	0.9510	0.9746	1.0031	0.9686	1.0007	0.9885	0.9885	0.9885
Fuel Cost ($/h)	**799.298**	803.194	799.6455	799.621	807.193	802.2744	800.144	806.088	801.240	800.5791	808.1031	802.2618
VD (p.u)	0.9024	**0.1280**	0.4182	0.6354	0.1202	0.1639	0.7375	0.1282	0.2878	0.8755	0.1455	0.2941

Bold values are show the results clearly found

41655.984 ($/h) and 0.6052 (p.u.), respectively. This case is compared with QOTLBO. The comparison of this case is illustrated in Table 11.

4.2.3 Case 6: fuel cost, power losses, and voltage deviation

All objective functions (fuel cost, power losses, voltage deviation) are taken into consideration simultaneously for optimization. The best non-domination combination of three objectives is 42338.39 ($/h), 12.1451 (MW), and 0.8059 (p.u.), respectively, and the minimum of each objectives is 41628.522 ($/h), 9.2175 (MW), and 0.6449 p.u.), as given in Table 12. Pareto front is shown in Fig. 10. The results are assessed to MODE, SPEA, and MALO as shown in Table 13.

4.3 IEEE 118-bus power system

The IEEE 118-bus test system has 118 buses, 54 generators (slack generator is at bus 69), 186 branches, 14 shunt elements, 9 transformers tap, and 130 control variables. Voltage, transformers tap, and shunt capacitors limits are considered in the range of [0.95–1.1]p.u., [0.9–1.1]p.u., and [0–25]p.u., respectively. The active and reactive power demands are 4242 MW and 1439 MVAr, respectively. Bus and line data can be found in [58].

4.3.1 Case 7: fuel cost and power losses

The optimization in this case takes into account two objectives fuel cost, and real power. Table 14 tabulates the results, the values of minimization objectives are 135,620.99 ($/h) and 23.15116 (MW), and the compromise solution is 138,669.21 ($/h) and 37.79042 (MW), respectively. Figure 11 shows the Pareto front.

4.3.2 Case 8: fuel cost and voltage deviation

In Case 8, fuel costs minimization and voltage deviation are taken into consideration. The simulation results of this

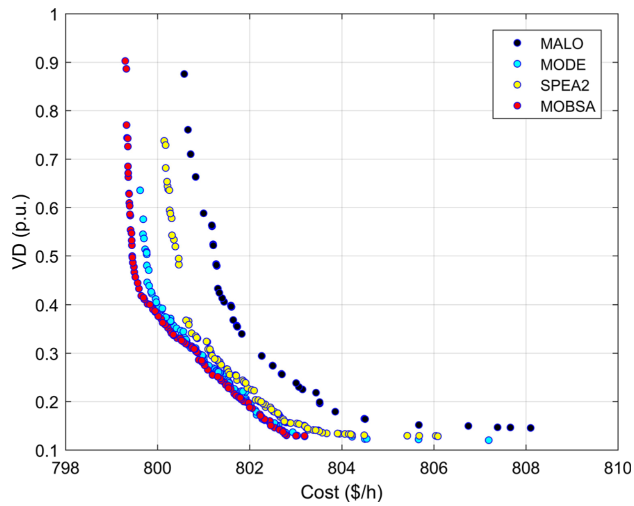

Fig. 6 Pareto fronts case 2

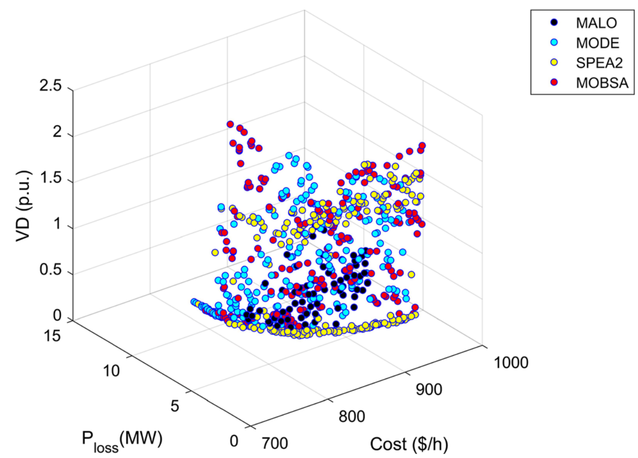

Fig. 7 Pareto fronts case 3

case are shown in Table 15, and its non-dominated solutions obtained are illustrated in Fig. 12. The proposed MOBSA

Table 7 Obtained solutions for the IEEE 30-bus power system case 3

Control variables	MOBSA			MODE			SPEA			MALO		
	Cost	Loss	VD	Cost	Loss	VD	Cost	Loss	VD	Cost	Loss	VD
P_{g2}	48.8136	80.0000	49.3915	48.8509	67.6215	77.9087	49.258	78.7031	62.8017	57.8554	57.8554	57.8553
P_{g5}	21.1947	50.000	20.7120	21.0170	49.9941	49.3692	21.0121	49.9898	37.6618	35.5101	35.5101	35.5101
P_{g8}	20.3833	35.000	25.8093	20.0562	34.4664	34.6300	19.4608	34.9919	31.8829	32.5252	32.5252	32.5252
P_{g11}	12.6728	30.000	17.2681	10.0806	29.3288	29.1944	10.9473	29.9153	29.3677	23.0593	23.0593	23.0593
P_{g13}	12.000	39.6442	18.8006	12.5262	39.6646	38.3200	12.1718	39.8777	27.5521	25.9671	25.9671	25.9671
V_{g1}	1.1000	1.1000	0.9928	1.0988	1.0997	1.0649	1.0933	1.0956	1.0064	1.0781	1.0781	1.0781
V_{g2}	1.0862	1.1000	1.0097	1.0862	1.0931	1.0523	1.0801	1.0890	0.9913	1.0658	1.0658	1.0658
V_{g5}	1.0570	1.0869	1.0190	1.0541	1.0762	1.0469	1.0501	1.0710	1.0196	1.0514	1.0514	1.0514
V_{g8}	1.0691	1.0935	1.0045	1.0705	1.0845	1.0514	1.0633	1.0799	1.0106	1.0504	1.0504	1.0504
V_{g11}	1.0532	1.1000	0.9957	1.0933	1.0929	1.0319	1.0818	1.0864	1.0047	1.0792	1.0792	1.0792
V_{g13}	1.0876	1.100	1.0418	1.0558	1.0961	1.0255	1.0932	1.0981	1.0314	1.0614	1.0614	1.0614
Q_{c10}	5.000	5.000	2.9370	4.4834	4.6148	4.6484	2.5962	4.1609	4.1072	3.4234	3.4234	3.4234
Q_{c12}	5.000	4.9208	3.9209	4.1881	4.2896	2.1895	3.2193	4.7388	5.0004	3.3161	3.3161	3.3161
Q_{c15}	3.9982	2.6675	4.1087	3.3571	3.8522	4.1630	4.5610	4.9121	4.0257	3.8335	3.8335	3.8335
Q_{c17}	5.000	5.000	2.6763	4.3256	3.3877	4.1380	4.6813	4.9452	1.6690	2.2129	2.2129	2.2129
Q_{c20}	4.8193	4.7180	5.000	4.5293	2.5493	0.3946	3.8813	4.9724	4.6849	3.0816	3.0816	3.0816
Q_{c21}	3.1741	4.9871	5.000	4.8810	4.1263	3.3329	3.5612	4.7594	4.8965	3.6278	3.6278	3.6278
Q_{c23}	2.4980	3.6872	5.000	4.9389	2.7826	3.2938	4.7364	4.7546	4.2525	2.9489	2.9489	2.9489
Q_{c24}	5.000	5.000	5.000	4.2225	4.4290	1.5732	4.8459	4.9460	4.6872	3.2768	3.2768	3.2768
Q_{c29}	1.5360	2.8688	2.2155	4.3234	2.9532	3.4505	0.5689	2.7648	1.0570	2.9224	2.9224	2.9224
T_{11}	1.1000	1.0751	1.0072	0.9552	1.0064	1.0793	1.0164	1.0106	0.9934	1.0546	1.0546	1.0546
T_{12}	0.9000	0.900	0.900	1.0821	0.9828	0.9088	0.9482	1.0092	0.9314	1.0258	1.0258	1.0258
T_{15}	1.0733	0.9865	1.0452	0.9776	1.0197	1.0348	1.0125	1.0268	1.0105	1.0251	1.0251	1.0251
T_{36}	0.9899	0.9945	0.9615	0.9638	0.9951	1.0145	0.9849	0.9859	0.9482	0.9975	0.9975	0.9975
Fuel Cost ($/h)	**799.271**	966.1605	811.988	799.693	941.128	954.611	799.596	963.936	866.341	808.545	905.863	856.981
P_{loss} (MW)	8.6795	**2.8589**	10.2673	8.9806	3.0682	3.4561	8.9612	2.9336	5.9422	7.1044	3.6991	6.0398
VD (p.u)	1.1483	2.0509	**0.0959**	1.4046	1.6804	0.3741	1.3863	1.6900	0.1041	0.4122	1.0201	0.1326

Bold values are show the results clearly found

Table 8 Obtained solutions for the IEEE 57-bus power system case 4

Control variables	Case 4		
	Cost	Loss	BCS
P_{g2}	77.0239	94.0699	36.0022
P_{g3}	44.9514	45.6990	103.9675
P_{g6}	71.3756	76.7565	82.6348
P_{g8}	422.1359	462.877	328.0784
P_{g9}	99.3348	84.0701	100.00
P_{g12}	40.5213	35.9403	410.00
V_{g1}	1.1000	1.0973	1.0976
V_{g2}	1.1000	1.1000	1.0976
V_{g3}	1.0911	1.0934	1.0975
V_{g6}	1.0982	1.0979	1.0973
V_{g8}	1.1000	1.1000	1.0943
V_{g9}	1.1000	1.0957	1.0909
V_{g12}	1.0936	1.0863	1.0882
Q_{c18}	11.0159	11.1071	8.8004
Q_{c25}	14.3268	15.4730	11.3439
Q_{c53}	13.3376	8.1177	13.6016
T_{19}	1.0891	1.0864	1.0854
T_{20}	1.0254	1.0054	1.0316
T_{31}	1.1000	1.0660	1.0220
T_{35}	1.0887	1.0824	1.0913
T_{36}	1.0790	1.0356	0.9000
T_{37}	1.1000	1.0970	1.0515
T_{41}	1.0176	1.0212	1.0582
T_{46}	1.0374	0.9623	0.9522
T_{54}	0.9000	0.9059	0.9000
T_{58}	0.9303	0.9500	1.0163
T_{59}	0.9231	0.9594	1.0083
T_{65}	0.9466	0.9769	1.0113
T_{66}	0.9000	0.9150	0.9722
T_{71}	0.9000	0.9000	1.1000
T_{73}	0.9931	0.9815	1.0558
T_{76}	0.9680	0.9853	0.9000
T_{80}	1.0649	1.0563	1.0854
Fuel Cost ($/h)	**41623.292**	44246.85	41959.152
P_{loss} (MW)	13.3806	**8.5788**	9.7667

Bold values are show the results clearly found

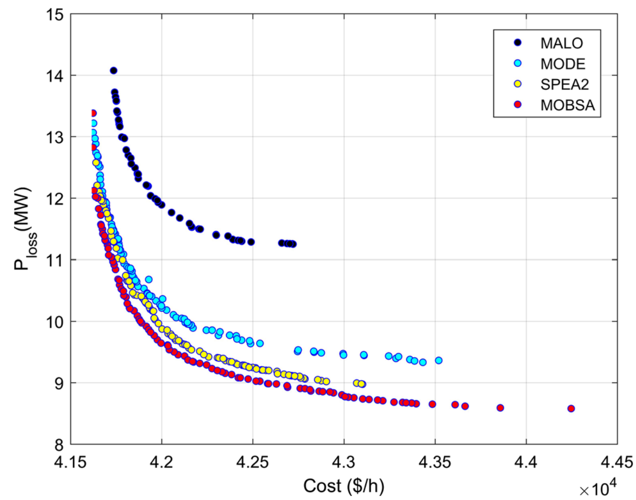

Fig. 8 Pareto fronts case 4

Table 9 Comparison solutions with other approaches for IEEE 57-bus case 4

Approaches	Objective functions	Cost	Loss
MOBSA	Min Cost	**41623.292**	13.3806
	Min Loss	44246.85	**8.5788**
	BCS	**41959.152**	**9.7667**
MODE	Min Cost	41623.602	13.0642
	Min Loss	43433.117	9.3315
	BCS	42000.426	10.2150
SPEA	Min Cost	41639.546	12.5753
	Min Loss	43101.856	8.9751
	BCS	42002.083	9.8733
MALO	Min Cost	41736.254	14.0741
	Min Loss	42720.771	11.2494
	BCS	41963.836	11.9884
QOTLBO [60]	Min Cost	-	-
	Min Loss	–	–
	BCS	42006.14	12.3669

Bold values are show the results clearly found

gives minimum cost and voltages deviation of 135839.01 ($/h) and 0.223 (p.u.), respectively. The BCSs are 136353.82 (MW), and 0.2787 (p.u.).

Discussion

This section visualizes the performance and efficacy of the proposed algorithm MOBSA in solving multi-objective optimal power flow problem. As we discuss before, standard BSA and its variants have been successfully evaluated in solving real-world problem. Similarly, in the current paper, the multi-objective BSA was performed in all cases. To better handle such multi-objective problem, two main challenging goals are required: accurate convergence towards the global optimum and high coverage (uniform distribution optimal front). More precisely, an effective algorithm should balance between convergence and coverage.

For results assessment, three most well-regarded algorithms are designated and re-implemented such as MALO, MODE, and SPEA-II. It is worth noticing that according to no free lunch theorem (NFL) [61] (Wolpert-Macready,1997),

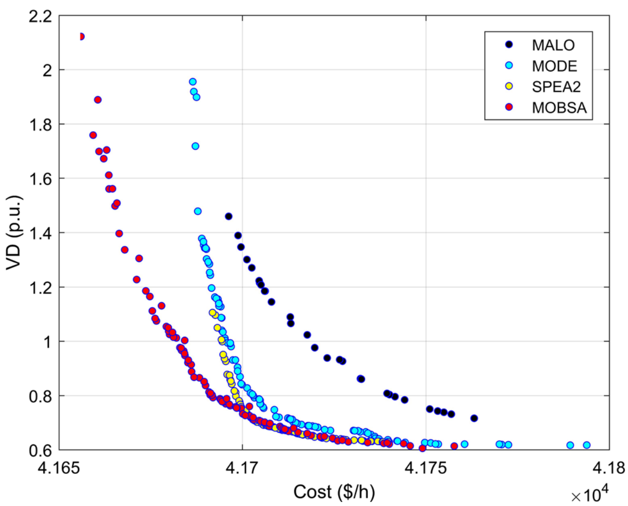

Fig. 9 Pareto fronts case 5

none of the meta-heuristics algorithms can be talented to resolve all optimization problems, and that is the main reason that some algorithms outperform others in addition to coverage and convergence.

It is worth discussing here that due to the dual populations, MOBSA can ensure different search directions, which leads to higher diversification in search space during optimization. Additionally, MOBSA highly boosts exploitation using the F parameter. Referring to the results found, it is clearly seen that MOBSA was able to provide better solution than other approaches in terms of distribution and solutions quality. It might be seen from case 1 in Fig. 5 that the Pareto optimal front of all algorithms is slightly similar except MALO.

Inspecting Pareto optimal fronts obtained for other cases, it is illustrated that MOBSA keeps a well-distributed and a good convergence characteristics, while the other multi-objective algorithms tend to converge to a local optimum, on account of the poor convergence to the Pareto optimal solutions. In particular, the MALO algorithm is not able to show good solutions in terms of convergence and coverage. However, when solving more complex problems, this algorithm can be easily stuck into local optima. Furthermore, additional important aspect of multi-objective optimization algorithms is the running time for achieving accurate optimal solutions. As illustrated in Table 16, it is clearly observed that the execution time of MOBSA is less than other algorithms.

To sum up, these results highly demonstrate that the algorithm suggested in this work MOBSA can find an approximate Pareto optimal solutions with high convergence and coverage along both objectives when solving complex problems in large scale.

Table 10 Obtained solutions for the IEEE 57-bus power system case 5

Control variables	Case 5		
	Cost	VD	BCS
P_{g2}	87.3182	83.6272	89.1329
P_{g3}	43.7329	46.1360	47.9784
P_{g6}	73.0293	73.5333	74.4954
P_{g8}	461.184	457.228	458.564
P_{g9}	99.2313	95.1478	91.1740
P_{g12}	361.294	363.564	358.803
V_{g1}	1.0579	1.0148	1.0174
V_{g2}	1.0592	1.0211	1.0210
V_{g3}	1.0473	1.0124	1.0152
V_{g6}	1.0724	0.9967	1.0104
V_{g8}	1.0821	1.0195	1.0377
V_{g9}	1.0732	1.0263	1.0268
V_{g12}	1.0531	1.0022	1.0081
Q_{c18}	17.1546	13.7511	9.8923
Q_{c25}	11.8311	15.4188	14.6095
Q_{c53}	16.3053	19.4996	17.5875
T_{19}	1.0907	1.0245	0.9979
T_{20}	0.9725	1.0004	0.9950
T_{31}	1.0125	0.9728	0.9751
T_{35}	1.0226	0.9929	1.0016
T_{36}	1.0012	1.0451	1.0045
T_{37}	1.0181	1.0052	1.0135
T_{41}	0.9985	0.9885	0.9933
T_{46}	0.9616	0.9304	0.9421
T_{54}	0.9173	0.9057	0.9021
T_{58}	0.9597	0.9364	0.9482
T_{59}	0.9566	0.9511	0.9644
T_{65}	0.9671	0.9848	0.9874
T_{66}	0.9421	0.9079	0.9088
T_{71}	0.9730	0.9497	0.9511
T_{73}	0.9736	1.0264	1.0296
T_{76}	0.9768	0.9037	0.9182
T_{80}	1.0065	1.0043	1.0123
Fuel Cost ($/h)	**41655.984**	41749.079	41721.309
VD (p.u)	2.1219	**0.6052**	0.6462

Bold values are show the results clearly found

Conclusion

The present paper proposes a novel evolutionary algorithm named MOBSA for solving multi-objective problems and finding Pareto optimal solutions. This algorithm was applied for different systems of transmission power systems, as IEEE 30-bus, IEEE 57-bus, and IEEE 118-bus systems, to minimize fuel cost, active power losses, and voltage deviation as objective functions. The obtained non-dominated solutions

Table 11 Comparison solutions with other approaches for IEEE 57-bus case 5

Approaches	Objective functions	Cost	VD
MOBSA	Min Cost	**41655.984**	2.1219
	Min VD	41749.079	0.6052
	BCS	**41721.309**	**0.6462**
MODE	Min Cost	41686.474	1.9553
	Min VD	41793.865	0.6167
	BCS	41722.405	0.6740
SPEA	Min Cost	41691.86	1.1054
	Min VD	41740.036	0.6283
	BCS	41721.653	0.6408
MALO	Min Cost	41696.259	1.4590
	Min VD	41763.187	0.7159
	BCS	41723.108	0.9382
QOTLBO [60]	Min Cost	-	-
	Min VD	–	–
	BCS	41758	0.6694

Bold values are show the results clearly found

Table 12 Obtained solutions for the IEEE 57-bus power system case 6

Control variables	Case 5			
	Cost	Loss	VD	BCS
P_{g2}	94.0699	30.000	100.00	100.00
P_{g3}	45.6990	136.342	140.00	68.379
P_{g6}	76.7565	99.8221	42.9389	100.00
P_{g8}	462.877	309.509	320.035	340.474
P_{g9}	84.0701	99.2145	30.000	97.844
P_{g12}	359.403	109.906	389.652	410.00
V_{g1}	1.0973	1.1000	1.0190	1.0309
V_{g2}	1.1000	1.1000	1.0394	1.0395
V_{g3}	1.0934	1.1000	1.0536	1.0329
V_{g6}	1.0979	1.0988	0.9902	1.0159
V_{g8}	1.1000	1.1000	1.0216	1.0399
V_{g9}	1.0957	1.0982	1.0201	1.0145
V_{g12}	1.0863	1.0987	1.0014	1.0176
Q_{c18}	11.1071	16.8920	8.9133	13.282
Q_{c25}	15.4730	15.1067	12.3928	10.499
Q_{c53}	8.1177	13.4005	13.2041	7.4401
T_{19}	1.0864	1.0939	1.0784	1.1000
T_{20}	1.0054	1.0384	0.9949	0.9536
T_{31}	1.0660	1.0947	0.9665	0.9746
T_{35}	1.0824	1.0844	0.9442	0.9704
T_{36}	1.0356	0.900	1.0115	0.9679

Table 12 continued

Control variables	Case 5			
	Cost	Loss	VD	BCS
T_{37}	1.0970	1.100	1.0238	1.0229
T_{41}	1.0212	1.0537	0.9679	0.9647
T_{46}	0.9623	0.900	0.9426	0.9319
T_{54}	0.9059	0.900	0.9000	0.9000
T_{58}	0.9501	0.9554	0.9647	0.9569
T_{59}	0.9594	0.9533	0.9700	0.9629
T_{65}	0.9769	0.9675	0.9875	1.0001
T_{66}	0.9150	0.9230	0.9115	0.9533
T_{71}	0.9000	0.9649	0.9574	0.9226
T_{73}	0.9815	0.9759	1.0079	1.0472
T_{76}	0.9853	1.0088	0.9249	0.9068
T_{80}	1.0563	1.0781	0.9935	1.0030
Fuel Cost ($/h)	**41628.522**	44566.334	45781.010	42338.390
P_{loss} (MW)	14.0890	**9.2175**	18.7484	12.1451
VD (p.u)	4.0986	4.3014	**0.6449**	0.8059

Bold values are show the results clearly found

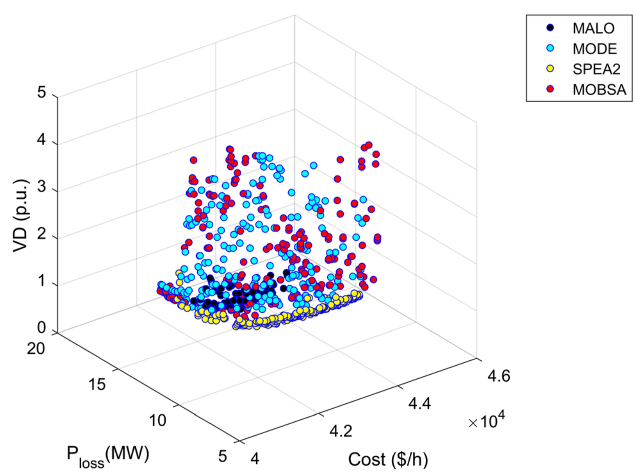

Fig. 10 Pareto fronts case 6

of MOBSA are compared with several multi-objective methods reported in the recent literature. Moreover, a fuzzy-based mechanism is employed to extract the best compromise solution. As the simulation results indicated, the multi-objective backtracking search algorithm is an efficient and a potential approach, and is successful in solving multi-objective optimal power flow compared with other methods like MODE, SPEA, MALO, MOABC/D, NSGA-II, and QOTLBO. To conclude, MOBSA is a robust and reliable optimization approach for solution of a large-scale multi-objective optimal power flow issue.

Table 13 Comparison solutions with other approaches for IEEE 57-bus case 6

Approaches	Objective functions	Cost	Loss	VD
MOBSA	Min Cost	**41628.522**	14.089	4.0986
	Min Loss	44566.334	**9.2175**	4.3014
	Min VD	45781.01	18.7484	**0.6449**
	BCS	42338.39	12.1451	0.8059
MODE	Min Cost	41641.799	14.3129	3.4120
	Min Loss	44550.885	9.6232	3.0861
	Min VD	42000.507	16.2763	0.7192
	BCS	42156.799	12.2357	1.0742
SPEA	Min Cost	41689.923	15.4866	1.4652
	Min Loss	44518.189	10.2569	1.0095
	Min VD	44425.098	12.0867	0.6476
	BCS	42392.541	11.3757	0.7558
MALO	Min Cost	41752.666	14.0091	2.0411
	Min Loss	42730.227	11.3397	17.4503
	Min VD	42145.358	14.5676	0.7422
	BCS	42125.629	12.7586	10.7878

Bold values are show the results clearly found

Table 14 Obtained solutions for the IEEE 118-bus power system case 7

Control variables	Case 7			Control variables			
	Cost	Loss	BCS		Cost	Loss	BCS
P_{g4}	30.0000	60.1793	41.2653	V_{g31}	0.95023	0.95017	0.95000
P_{g6}	30.0131	30.0000	30.1264	V_{g32}	0.95005	0.95002	0.95005
P_{g8}	30.0000	76.8729	38.1097	V_{g34}	0.95084	0.95252	0.95178
P_{g10}	30.0129	35.2858	32.5711	V_{g36}	0.95000	0.95003	0.95001
P_{g12}	324.687	165.000	232.786	V_{g40}	0.95000	0.95252	0.95073
P_{g15}	68.9445	104.853	90.4106	V_{g42}	0.95001	0.95005	0.95002
P_{g18}	30.1649	58.1878	38.3610	V_{g46}	0.95000	0.95033	0.95008
P_{g19}	35.9830	35.3255	44.9259	V_{g49}	0.96515	0.95534	0.95707
P_{g24}	30.0000	92.5431	51.0438	V_{g54}	0.95000	0.95079	0.95000
P_{g25}	30.0000	30.2401	30.3803	V_{g55}	0.95000	0.95168	0.95061
P_{g26}	134.543	96.0000	103.8591	V_{g56}	0.95000	0.95024	0.95016
P_{g27}	224.5519	124.2141	151.4122	V_{g59}	0.96247	0.95109	0.95968
P_{g31}	30.0000	52.1126	39.4980	V_{g61}	0.95227	0.95415	0.95688
P_{g32}	32.1051	32.1157	32.1487	V_{g62}	0.95521	0.95000	0.95256
P_{g34}	30.0000	70.1493	41.4697	V_{g65}	0.95000	0.95000	0.95006
P_{g36}	30.0000	64.822	38.9066	V_{g66}	0.95013	0.95429	0.95260
P_{g40}	30.0000	34.9128	38.9772	V_{g69}	0.95488	0.95215	0.95334
P_{g42}	30.0000	100.000	79.7534	V_{g70}	0.95000	0.95000	0.95000
P_{g46}	30.0000	94.0166	89.7830	V_{g72}	0.95021	0.95438	0.95029
P_{g49}	35.7000	35.7000	36.1268	V_{g73}	0.95003	0.95053	0.95010
P_{g54}	176.359	146.391	157.530	V_{g74}	0.95007	0.95000	0.95010
P_{g55}	44.4000	148.000	56.5203	V_{g76}	0.95005	0.95066	0.95000
P_{g56}	30.0000	99.2247	94.0065	V_{g77}	0.95000	0.95007	0.950015
P_{g59}	30.0000	100.000	97.9837	V_{g80}	0.95188	0.95138	0.95151
P_{g61}	118.790	218.113	154.952	V_{g85}	0.95427	0.95000	0.95226
P_{g62}	133.367	78.4337	114.029	V_{g87}	0.95680	0.96343	0.96150

Table 14 continued

Control variables	Case 7			Control variables			
	Cost	Loss	BCS		Cost	Loss	BCS
P_{g65}	30.0000	34.8942	30.1782	V_{g89}	0.95033	0.95203	0.95138
P_{g66}	273.248	147.300	260.789	V_{g90}	0.95000	0.95000	0.95020
P_{g69}	287.162	147.600	219.761	V_{g91}	0.95000	0.95000	0.95000
P_{g70}	30.3594	30.3514	30.1358	V_{g92}	0.95000	0.95003	0.95001
P_{g72}	30.2032	30.0000	30.0654	V_{g99}	0.95331	0.95109	0.95362
P_{g73}	30.0000	32.4568	30.2021	V_{g100}	0.95000	0.95000	0.95000
P_{g74}	30.6347	72.9019	46.8355	V_{g103}	0.95386	0.95000	0.95150
P_{g76}	30.0000	99.7440	76.2120	V_{g104}	0.95000	0.95182	0.95014
P_{g77}	30.0000	100.000	38.2109	V_{g105}	0.95000	0.95000	0.95000
P_{g80}	35.5586	314.949	317.922	V_{g107}	0.95014	0.95044	0.95013
P_{g85}	30.1061	35.0047	30.1285	V_{g110}	0.95019	0.95034	0.95033
P_{g87}	31.2000	31.3309	31.2021	V_{g111}	0.95000	0.95048	0.95029
P_{g89}	375.178	212.100	278.570	V_{g112}	0.95000	0.95002	0.95003
P_{g90}	30.0000	100.000	37.7915	V_{g113}	0.95000	0.95000	0.95000
P_{g91}	30.0000	30.0000	30.3881	V_{g113}	0.95196	0.95000	0.95138
P_{g92}	30.4082	30.1882	30.3144	Q_{c5}	3.38550	1.61976	2.52518
P_{g99}	30.0000	35.3390	32.7408	Q_{c34}	5.32615	2.82468	4.49088
P_{g100}	175.950	122.893	174.423	Q_{c37}	2.42953	16.3544	9.00684
P_{g103}	42.2206	43.2168	43.2486	Q_{c44}	11.7935	0.00000	12.1570
P_{g104}	30.0779	35.2410	30.9248	Q_{c45}	0.29473	8.91632	4.10189
P_{g105}	30.0000	40.3559	34.5829	Q_{c46}	5.05121	2.11643	3.12907
P_{g107}	30.3799	53.6548	38.3505	Q_{c48}	9.03098	4.20223	10.9424
P_{g110}	30.0000	34.6223	30.4602	Q_{c74}	10.4224	3.02360	7.21445
P_{g111}	40.8000	40.9069	40.9773	Q_{c79}	6.26478	6.94610	11.8837
P_{g112}	30.0000	38.5924	34.2614	Q_{c82}	4.82128	15.9247	22.7880
P_{g113}	30.0000	39.9421	31.8849	Q_{c83}	0.00000	23.1907	10.8083
P_{g116}	30.0000	30.0000	30.3280	Q_{c105}	3.20657	8.05024	4.13828
V_{g1}	0.9500	0.9501	0.95000	Q_{c107}	0.00000	13.2519	6.25001
V_{g4}	0.9501	0.9501	0.95010	Q_{c110}	0.72215	18.7091	8.49107
V_{g6}	0.95302	0.95659	0.95472	T_8	0.93277	1.00032	0.98050
V_{g8}	0.95023	0.95135	0.95110	T_{32}	0.94733	1.01954	1.04934
V_{g10}	0.95011	0.95019	0.95098	T_{36}	0.97501	0.96124	0.96801
V_{g12}	0.95000	0.95000	0.95001	T_{51}	0.97404	0.95117	0.97532
$V_{g\ 15}$	0.95000	0.95000	0.95000	T_{93}	0.90629	0.95705	0.93581
V_{g18}	0.95000	0.95059	0.95009	T_{95}	1.01518	1.00230	0.99789
V_{g19}	0.95000	0.95183	0.95077	T_{102}	0.90000	0.98070	0.94320
V_{g24}	0.95000	0.95000	0.95245	T_{107}	0.91640	0.92551	0.92432
V_{g25}	0.96749	0.95036	0.95813	T_{127}	0.90000	0.94356	0.97994
V_{g26}	0.95004	0.95000	0.95016	Fuel Cost ($/h)	**135620.99**	147577.9	**138669.21**
V_{g27}	0.95590	0.95122	0.95117	P_{loss} (MW)	73.71883	**23.15116**	**37.79042**

Bold values are show the results clearly found

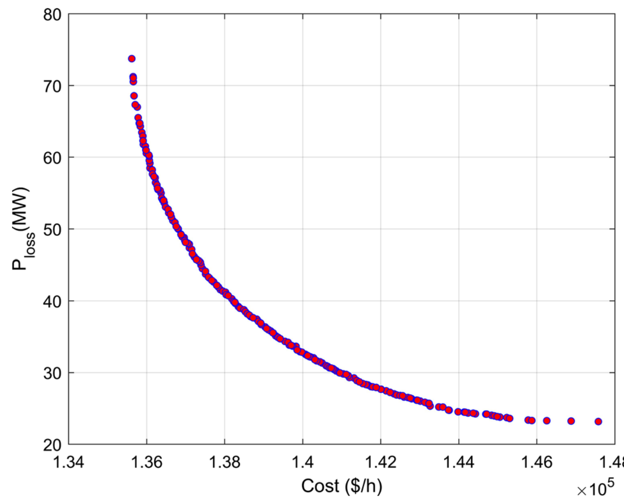

Fig. 11 Pareto front case 7

Table 15 Obtained solutions for the IEEE 118-bus power system case 8

Control variables	Case 8		Control variables		
	Cost	VD		Cost	VD
P_{g4}	30.5462	38.8024	V_{g31}	0.9797	0.9975
P_{g6}	30.0000	36.3103	V_{g32}	0.9875	0.9992
P_{g8}	34.7139	30.9273	V_{g34}	0.9855	1.0045
P_{g10}	30.0000	49.8454	V_{g36}	0.9838	0.9964
P_{g12}	302.820	22.0928	V_{g40}	0.9981	1.0073
P_{g15}	67.3579	75.3020	V_{g42}	0.9713	1.0048
P_{g18}	39.8719	49.8056	V_{g46}	0.9809	0.9880
P_{g19}	30.2845	30.0000	V_{g49}	1.0091	1.0135
P_{g24}	30.0812	47.5201	V_{g54}	0.9875	1.0228
P_{g25}	35.3232	33.6235	V_{g55}	0.9792	0.9903
P_{g26}	142.692	11.3177	V_{g56}	0.9890	1.0108
P_{g27}	211.687	16.5952	V_{g59}	1.0115	1.0197
P_{g31}	33.2950	39.6022	V_{g61}	0.9890	1.0185
P_{g32}	32.1013	32.1000	V_{g62}	0.9590	0.9580
P_{g34}	32.8077	51.2867	V_{g65}	1.0131	1.0160
P_{g36}	30.0497	57.6172	V_{g66}	1.0416	1.0479
P_{g40}	32.6218	40.1293	V_{g69}	1.0185	1.0136
P_{g42}	34.3162	57.3848	V_{g70}	1.0113	0.9997
P_{g46}	33.2325	38.7800	V_{g72}	1.0059	1.0022
P_{g49}	35.7000	42.3636	V_{g73}	1.0044	0.9978
P_{g54}	148.476	163.052	V_{g74}	1.0196	1.0129
P_{g55}	45.7630	48.3386	V_{g76}	0.9681	0.9918
P_{g56}	30.0000	44.2482	V_{g77}	1.0007	1.0027
P_{g59}	35.7226	50.2249	V_{g80}	1.0141	1.0226
P_{g61}	135.619	140.897	V_{g85}	1.0109	1.0116
P_{g62}	136.749	120.1611	V_{g87}	0.9679	0.9990

Table 15 continued

Control variables	Case 8		Control variables		
	Cost	VD		Cost	VD
P_{g65}	30.2030	36.2847	V_{g89}	1.0064	1.0006
P_{g66}	279.516	224.630	V_{g90}	0.9996	0.9804
P_{g69}	284.352	307.584	V_{g91}	1.0195	1.0095
P_{g70}	30.0000	43.4691	V_{g92}	1.0084	1.0128
P_{g72}	30.2862	30.0000	V_{g99}	0.9758	0.9531
P_{g73}	30.1156	31.6706	V_{g100}	0.9976	1.0187
P_{g74}	30.3171	30.3578	V_{g103}	0.9876	0.9862
P_{g76}	31.9881	35.6065	V_{g104}	0.9660	1.0004
P_{g77}	30.4159	34.0665	V_{g105}	0.9801	0.9805
P_{g80}	343.484	577.000	V_{g107}	0.9913	1.1000
P_{g85}	30.0000	35.8900	V_{g110}	1.0060	1.0262
P_{g87}	31.2315	31.2000	V_{g111}	0.9620	0.9785
P_{g89}	385.730	247.777	V_{g112}	1.0038	0.9873
P_{g90}	30.0000	33.7837	V_{g113}	1.0156	0.9602
P_{g91}	30.0000	40.9193	V_{g113}	0.9969	1.0022
P_{g92}	30.0000	44.3722	Q_{c5}	9.3782	8.3015
P_{g99}	33.6681	37.8211	Q_{c34}	8.8518	13.6746
P_{g100}	164.083	167.1058	Q_{c37}	6.8163	2.5103
P_{g103}	42.7060	54.3541	Q_{c44}	11.488	19.4873
P_{g104}	30.9303	31.6251	Q_{c45}	22.4924	25.000
P_{g105}	30.0000	33.4794	Q_{c46}	17.1545	16.8897
P_{g107}	32.1084	41.0981	Q_{c48}	7.4753	3.4575
P_{g110}	30.9871	30.0000	Q_{c74}	12.709	18.8601
P_{g111}	41.2411	45.3562	Q_{c79}	2.1015	15.4595
P_{g112}	31.9849	37.8591	Q_{c82}	15.6375	19.7248
P_{g113}	31.0626	34.2657	Q_{c83}	18.4274	15.2675
P_{g116}	31.2005	56.0237	Q_{c105}	9.5776	6.0153
V_{g1}	0.9955	0.9972	Q_{c107}	17.286	1.8649
V_{g4}	0.9848	0.9929	Q_{c110}	20.0789	23.0504
V_{g6}	0.9769	0.9915	T_8	0.9958	0.9560
V_{g8}	0.9817	0.9775	T_{32}	0.9797	0.9761
V_{g10}	1.0019	1.0019	T_{36}	0.9947	0.9683
V_{g12}	0.9997	1.0122	T_{51}	0.9729	0.9596
V_{g15}	1.0197	1.0215	T_{93}	1.0279	0.9861
V_{g18}	1.0324	0.9851	T_{95}	0.9353	0.9556
V_{g19}	1.0239	1.0301	T_{102}	1.0435	0.9401
V_{g24}	1.0058	0.9636	T_{107}	0.9256	0.9155
V_{g25}	1.0239	1.0588	T_{127}	0.9563	0.9624
V_{g26}	0.9905	1.0560	Fuel Cost ($/h)	**135839.01**	141210.36
V_{g27}	1.0118	1.0118	VD (p.u.)	0.6489	**0.2229**

Bold values are show the results clearly found

Table 16 Execution times

	MOBSA	MODE	SPEA	MALO
Case 1	**118.60**s	130.71s	160.45s	149.02s
Case 2	118.55s	**117.58**s	145.01s	131.31s
Case 3	**126.68**s	132.12s	152.40s	148.92s
Case 4	**202.18**s	203.58s	257.16s	235.74s
Case 5	205.65s	**202.77**s	253.04s	238.91s
Case 6	**206.06**s	214.86s	262.46s	239.74s

Bold values are show the results clearly found

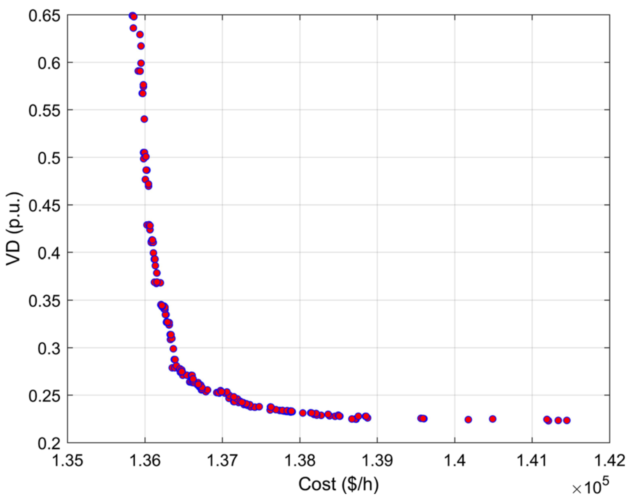

Fig. 12 Pareto front case 8

Compliance with ethical standards

Conflict of interest The authors declare that they have no conflict of interest.

References

1. Dommel HW, Tinney WF (1968) Optimal power flow solutions. IEEE Trans Power Syst 87(10):1866–1876
2. Syai'in M, Soeprijanto A (2012) Improved algorithm of Newton Raphson power flow using GCC limit based on neural network. Int J Electr Comput Sci 12(1):7–12
3. Al Ameri A, Nichita C, Dakyo B (2014) An efficient algorithm for power load flow solutions by schur complement and threshold technique. Int J Adv Res Electr Electrical Inst Eng 3(8):11062–11069
4. Singhal K (2014) Comparison between load flow analysis methods in power system using MATLAB. Int J Sci Eng Res 5(5):1412–1419
5. Habibollahzadeh H, Luo GX, Semlyen (1989) A Hydrothermal optimal power flow based on a combined linear and nonlinear programming methodology. IEEE Trans Power Syst 4(2):530–537
6. Aoki K, Nishikori A, Yokoyama RT (1987) Constrained load flow using recursive quadratic programming. IEEE Trans Power Syst 2(1):8–16
7. Momoh JA, Zhu JZ (1999) Improved interior point method for OPF problems. IEEE Trans Power Syst 14(3):1114–1120
8. Salgado RS, Schiochet AF, Barboza LV (2010) Multi-objective optimal power flow solutions through a parameterized model. In: Eighth world energy system conference, Valahia, Romania
9. Hayyolalam V, Pourhaji Kazem AA (2020) Black Widow Optimization Algorithm: a novel meta-heuristic approach for solving engineering optimization problems. Eng Appl Artif Intell 87:103249
10. Mirjalili S, Gandomi AH, Mirjalili SZ, Saremi S, Faris H, Mirjalili SM (2017) Salp Swarm algorithm: a bio-inspired optimizer for engineering design problems. Adv Eng Softw 114:163–191
11. Kamboj VK, Nandi Y, Bhadoria A, Sehgal S (2020) An intensify Harris hawks optimizer for numerical and engineering optimization problems. Appl Soft Comput 89:106018
12. Dhawale D, Kamboj VK (2020) hHHO–IGWO: A new Hybrid Harris Hawks optimizer for solving global optimization problems. International Conference on Computation, Automation and Knowledge Management (ICCAKM) 19495342
13. Hashim FA, Houssein EH, Mabrouk MS, Al-Atabany W, Mirjalili S (2019) Henry gas solubility optimization: A novel physics-based algorithm. Future Gener Comput Syst 101:646–667
14. Bhadoria A, Kamboj VK (2018) Optimal generation scheduling and dispatch of thermal generating units considering impact of wind penetration using hGWO-RES algorithm. Appl Intell 49(4):1517–1547
15. Weiguo Z, Zhang Z, Wang L (2020) Manta ray foraging optimization: an effective bio-inspired optimizer for engineering applications. Eng Appl Artif Intell 87:103300
16. Abou El Ela AA, Abido MA, Spea SR (2011) Differential evolution algorithm for optimal reactive power dispatch. Electr Power Syst Res 81(2):458–464
17. Suresh V, Sreejith S, Sudabattula SK, Kamboj VK (2019) Demand response-integrated economic dispatch incorporatingrenewable energy sources using ameliorated dragonfly algorithm. Electr Eng 101(2):421–442
18. Abuella M, Hatziadoniu J (2016) Selection of most effective control variables for solving optimal power flow using sensitivity analysis in particle swarm algorithm. arXiv:1601.04150
19. Allaoua B, Laouafi A (2008) Collective intelligence for optimal power flow solution using ant colony optimization. Electr J Pract Tech 7(13):88–105
20. Wankhade CM, Vaidya AP (2012) Optimal power flow evaluation of power system using genetic algorithm. Int J Power Syst Oper Energy Manag 1(4):2231–4407
21. Ara AL, Kazemi A, Behshad M (2013) Improving power systems operation through multi-objective optimal location of optimal unied power ow controller. Turk J Electr Eng Comput Sci 21:1893–1908
22. Narimani MR, Azizipanah-Abarghooee R, Zoghdar-Moghadam-Shahrekohne B, Gholami K (2013) A novel approach to multi-objective optimal power flow by a new hybrid optimization algorithm considering generator constraints and multi-fuel type. Energy 49(1):119–136
23. Sulaiman MH, Mustaffa Z, Mohamed MR, Aliman O (2015) Using the gray wolf optimizer for solving optimal reactive power dispatch problem. Appl Soft Comput 32:286–292
24. Attia AF, El Sehiemy RA, Hasanien HM (2018) Optimal power flow solution in power systems using a novel Sine-Cosine algorithm. Int J Electr Power Energy Syst 99:331–343
25. Ghaemi S, Aghdam FH, Safari A, Farrokhifar M (2019) Stochastic economic analysis of FACTS devices on contingent transmission networks using hybrid biogeography-based optimization. Electr Eng 101:829–843
26. Khorsandi A, Hosseinian SH, Ghazanfari A (2013) Modified artificial bee colony algorithm based on fuzzy multi-objective technique for optimal power flow problem. Electr Power Syst Res 95:206–213

27. Shang R, Wang J, Jiao L, Wang Y (2014) An improved decomposition-based memetic algorithm for multi-objective capacitated arc routing problem. Appl Soft Comput 19:343–361
28. Liang RH, Wu CY, Chen YT, Tseng WT (2015) Multi-objective dynamic optimal power flow using improved artificial bee colony algorithm based on Pareto optimization. Int Trans Electr Energy Syst 26(4):692–712
29. Medina AM, Das S, Carlos ACC, Ramirez MJ (2014) Decomposition-based modern metaheuristic algorithms for multi-objective optimal power flow a comparative study. Eng Appl Artif Intel 32:10–20
30. Ghasemi M, Ghavidel S, Ghanbarian MM, Gitizadeh M (2015) Multi-objective optimal electric power planning in the power system using Gaussian bare-bones imperialist competitive algorithm. Inf Sci 294:286–304
31. Yuan X, Zhang B, Wang P, Ji L, Yuan Y, Huang Y, Lei X (2017) Multi-objective optimal power flow based on improved strength Pareto evolutionary algorithm. Energy 122:70–82
32. Warida W, Hizama H, Mariuna N, Wahaba NIA (2018) A novel quasi-oppositional modified Jaya algorithm for multi-objective optimal power flow solution. Appl Soft Comput 65:360–373
33. Zhanga J, Tang Q, Li P, Deng D, Chen Y (2016) A modified MOEA/D approach to the solution of multi-objective optimal power flow problem. Appl Soft Comput 47:494–514
34. Sivasubramani S, Swarup K (2011) Multi-objective harmony search algorithm for optimal power flow problem. Int J Electr Power Energy Syst 33:745–752
35. Rahmati M, Effatnejad R, Safari A (2014) Comprehensive Learning Particle Swarm Optimization (CLPSO) for Multi-objective Optimal Power Flow. Indian J Sci Tech 7(3):262–270
36. Barocio E, Regalado J, Cuevas E, Uribe F, Zúñga P, Torres PJR (2017) Modified bio-inspired optimisation algorithm with a centroid decision making approach for solving a multi-objective optimal power flow problem. IET Gener Trans Distri 11(4):1012–1022
37. Abido MA, Al-Ali NA (2012) Multi-Objective Optimal Power Flow Using Differential Evolution. Arab J Sci Eng 37:991–1005
38. Shaheen AM, Farrag SM, El-Sehiemy RA (2017) A Novel Multi-Objective Optimal Power Flow Solution Methodology. IET Proceedings Gener Trans Distrib 11(2):570–581
39. Pulluri H, Naresh R, Sharma V (2017) An Enhanced Self-adaptive Differential Evolution Based Solution Methodology for Multiobjective Optimal Power Flow. Appl Soft Comput 54:229–245
40. Shaheen AM, El-Sehiemy RA, Farrag SM (2015) Solving multi-objective optimal power flow problem via forced initialised differential evolution algorithm. IET Gener Trans Distrib 10(7):1634–1647
41. Ghasemi M, Ghavidel S, Ghanbarian MM, Massrur HR, Gharibzadeh M (2014) Application of imperialist competitive algorithm with its modified techniques for multi-objective optimal power flow problem: a comparative study. Inf Sci 281:225–247
42. Civicioglu P (2013) Backtracking search optimization algorithm for numerical optimization problems. Appl Math Comput 219(15):8121–8144
43. Chatzipavlis A, Tsekouras GE, Trygonis V, Velegrakis AF, Tsimikas J, Rigos A, Hasiotis T, Salmas C (2019) Modeling beach realignment using a neuro-fuzzy network optimized by a novel backtracking search algorithm. Neural Comput Appl 31:1747–1763
44. Ahandani MA, Ghiasi AR, Kharrati H (2018) Parameter identification of chaotic systems using a shuffled backtracking search optimization algorithm. Soft Comput 22:8317–8339
45. Lu J, Ding J (2019) Construction of prediction intervals for carbon residual of crude oil based on deep stochastic configuration networks. Inf Sci 486:119–132
46. Khan WU, Ye Z, Chaudhary NI, Raja MAZ (2018) Backtracking search integrated with sequential quadratic programming for nonlinear active noise control systems. Appl Soft Comput 73:666–683
47. Thai V, Cheng J, Nguyen V, Daothi P (2019) Optimizing SVM's parameters based on backtracking search optimization algorithm for gear fault diagnosis. J Vibroeng 21(1):66–81
48. Sriram M, Ravindra K (2020) Backtracking Search Optimization Algorithm Based MPPT Technique for Solar PV System. in: Adv Decis Sci, Image Process, Secur Comput Vis, Springer 498–506
49. Abdolrasol MGM, Hannan MA, Mohamed A, Amiruldin UAU, Abidin IBZ, Uddin MN (2018) An optimal scheduling controller for virtual power plant and microgrid integration using the binary backtracking search algorithm. IEEE Trans Ind Appl 54:2834–2844
50. Shaheen AM, El-Sehiemy RA, Farrag SM (2016) Optimal reactive power dispatch using backtracking search algorithm. Aust J Electr Electron Eng 13:200–210
51. Chaib AE, Bouchekara H, Mehasni R, Abido MA (2016) Optimal power flow with emission and non-smooth cost functions using backtracking search optimization algorithm. Int J Electr Power Energy Syst 81:64–77
52. El-Fergany A (2016) Multi-objective allocation of multi-type distributed generators along distribution networks using backtracking search algorithm and fuzzy expert rules. Electric Power Compon Syst 44(3):252–267
53. Lin J (2019) Backtracking search based hyper-heuristic for the flexible job-shop scheduling problem with fuzzy processing time. Eng Appl Artif Intell 77:186–196
54. Badawy MM, Ali ZH, Ali HA (2019) QoS provisioning framework for service-oriented internet of things (IoT). Cluster Comput 1–17
55. Zadeh LA (1965) Fuzzy sets. Information and Control 8:338–353
56. Bellman R, Zadeh LA (1970) Decision-making in a fuzzy environment. Manage Sci 17:141–164
57. Alsac O, Stott B (1974) Optimal load flow with steady-state security. IEEE Trans Power Apparatus Syst 93(3):745–751
58. Zimmerman RD, Murillo-Sánchez CE, Thomas, RJ, Matpower Available at: http://www.pserc.cornell.edu/matpower
59. Bhowmik AR, Chakraborty AK (2014) Solution of optimal power flow using non-dominated sorting multi objective gravitational search algorithm. Int J Electr Power Energy Syst 62:323–334
60. Mandal B, Roy PK (2014) Multi-objective optimal power flow using quasi-oppositional teaching learning based optimization. Appl Soft Comput 21:590–606
61. Wolpert DH, Macready WG (1997) No free lunch theorems for optimization. Evol Comput IEEE Trans 1:67–82